J Ind Microbiol Biotechnol (2012) 39:255–268
DOI 10.1007/s10295-011-1023-7

ORIGINAL PAPER

# Global transcriptome analysis of the tetrachloroethene-dechlorinating bacterium *Desulfitobacterium hafniense* Y51 in the presence of various electron donors and terminal electron acceptors

**Xue Peng · Shogo Yamamoto · Alain A. Vertès · Gabor Keresztes · Ken-ichi Inatomi · Masayuki Inui · Hideaki Yukawa**

Received: 28 April 2011 / Accepted: 24 July 2011 / Published online: 23 August 2011


**Abstract** *Desulfitobacterium hafniense* Y51 is a dechlorinating bacterium that encodes an unusually large set of *O*-demethylase paralogs and specialized respiratory systems including specialized electron donors and acceptors. To use this organism in bioremediation of tetrachloroethene (PCE) or trichloroethene (TCE) pollution, expression patterns of its 5,060 genes were determined under different conditions using 60-mer probes in DNA microarrays. PCE, TCE, fumarate, nitrate, and dimethyl sulfoxide (DMSO) respiration all sustain the growth of strain Y51. Global transcriptome analyses were thus performed using various electron donor and acceptor couples (respectively, pyruvate and either fumarate, TCE, nitrate, or DMSO, and vanillate/fumarate). When TCE is used as terminal electron acceptor, resulting in its detoxification, a series of electron carriers comprising a cytochrome *bd*-type quinol oxidase (DSY4055-4056), a ferredoxin (DSY1451), and four Fe–S proteins (DSY1626, DSY1629, DSY0733, DSY3309) are upregulated, suggesting that the products of these genes are involved in PCE oxidoreduction. Interestingly, the PCE dehalogenase cluster (*pceABCT*) is constitutively expressed in the media tested, with *pceT* being upregulated and *pceC* downregulated in pyruvate/TCE-containing medium. In addition, another dehalogenation enzyme (DSY1155 coding for a putative chlorophenol reductive dehalogenase), is induced 225-fold in that medium, despite not being involved in PCE respiration. Remarkably since the reducing equivalents formed during pyruvate conversion to acetyl-CoA are channeled to electron acceptors including halogenated compounds, pyruvate induces expression of a pyruvate:ferredoxin oxidoreductase. This study paves the way to understanding the physiology of *D. hafniense*, optimizing this microbe as a bioremediation agent, and designing bioarray sensors to monitor the presence of dechlorinating organisms in the environment.

**Keywords** *Desulfitobacterium hafniense* · Bioremediation · Dechlorination · Dehalorespiration · Tetrachloroethene

X. Peng · S. Yamamoto · A. A. Vertès · G. Keresztes · K. Inatomi · M. Inui · H. Yukawa (✉)
Molecular Microbiology and Biotechnology Group, Research Institute of Innovative Technology for the Earth (RITE), 9-2 Kizugawadai, Kizugawa, Kyoto 619-0292, Japan
e-mail: mmg-lab@rite.or.jp

*Present Address:*
X. Peng
School of Life Sciences, Xuzhou Normal University, 101 Shanghai Road, Tongshan New District, Xuzhou 221116, Jiangsu, China

## Introduction

Tetrachloroethene (perchloroethene, PCE) and trichloroethene (TCE) are excellent solvents for dry cleaning, but their widespread use has caused large-scale environmental pollution. The remediation of PCE/TCE-contaminated sites has thus become an urgent issue worldwide [6]. Dehalorespiration, or bacterial growth coupled to the utilization of a chlorinated compound, is to date the only known biological mechanism for degrading highly halogenated compounds. In dehalorespiration, the oxidation of electron donors is coupled to the reduction, and detoxification, of halogenated organic compounds. Dehalorespiring bacteria therefore constitute a promising and cost-effective approach for the bioremediation of PCE-contaminated sites [38].

The two most prominent genera comprising species that dechlorinate a large array of chemical compounds, including halophenolic compounds and chloroalkenes, are *Dehalococcoides* [20] and *Desulfitobacterium* [43]. Species of both of these genera have been isolated from PCE-contaminated sites around the world and analyzed. For example, the complete genome sequence of *Dehalococcoides ethenogenes* strain 195 [36] reveals that this organism contains 17 putative dehalogenases but that it can only use hydrogen as electron donor and PCE as terminal electron acceptor, and requires acetate as a carbon source and cobalamin for dehalogenase activity [17, 36]. This process involves an Ni/Fe hydrogenase that splits hydrogen into protons and electrons [44], which are in turn consumed by the PCE dehalogenase. This mechanism has been investigated in detail. For example, two dehalorespiration-deficient mutants of *D. dehalogenans* have been constructed by Tn*916* insertion in the upstream region of the formate-hydrogen lyase (FHL) or Ni/Fe hydrogenase genes [37]. Similarly, hydrogen consumption with concomitant transfer of electrons to PCE was observed in *D. chlororespirans*, *Desulfuromonas*, and *Desulfomonile tiedjei* [14], confirming the central role played by hydrogenases in PCE degradation. Moreover, menaquinone has been reported to serve as an electron mediator of PCE reduction in *D. restrictus* [35]. On the basis of the above information, the predicted electron transfer chain of dehalogenation in these organisms is of the following form: formate $\rightarrow H_2 \rightarrow$ proton + electron $\rightarrow$ menaquinone (MQ) $\rightarrow\rightarrow$ PCE. What is more, if pyruvate is supplied as the electron donor, it can be split into formate by pyruvate-formate lyase (PFL) [10].

*Desulfitobacterium hafniense* Y51 is a strict anaerobe that was isolated in Japan from PCE-contaminated soil. As expected, this organism is capable of dechlorinating PCE via TCE to *cis*-1,2-dichloroethene (*cis*-DCE) [6, 40, 41]. The dehalogenase gene cluster (*pceABCT*) of strain Y51 is obviously important in dehalorespiration; remarkably, it is flanked by two nearly identical IS*Desp* (IS*256* family) transposable elements [6, 7] suggesting it was acquired by *D. hafniense* Y51 via horizontal DNA transfer [9, 18, 25]. However, no dehalogenase gene was found adjacent to the genes encoding electron chain proteins, thus making it difficult to identify the proteins that are directly linked to dehalogenases for electron transfer.

In parallel, *Dehalococcoides*-containing consortia have been tested for the bioremediation of contaminated sites with some success [19]. What makes strain Y51 particularly interesting is that it has a much broader range of electron donor and acceptor metabolism systems than *Dehalococcoides* [28]. This includes numerous sequences coding for dimethyl sulfoxide (DMSO), fumarate, nitrate, nitrite, sulfate, and sulfite reductases; this property may be ascribed to its much larger genome [28]. An additional remarkable feature is that *D. hafniense* Y51 contains a large number of *O*-demethylase analogs, which allow the utilization of lignin-derived phenyl methyl ethers as electron donors. As a preliminary to optimizing the bioremediation use of *D. hafniense* Y51 and to facilitate the study of the physiology of this microorganism, we confirmed by various growth experiments that the bacterial strain in our laboratory exhibited the expected phenotype, and investigated by global transcriptome analysis the expression levels of its main reductases and respiration genes.

## Materials and methods

### Strain and culture media

Strain Y51 is an isolate from a PCE-polluted soil sample collected in Fukuoka, Japan [40]. MMY (per liter: $K_2PO_4$, 7.8 g; $KH_2PO_4$, 1.2 g; sodium citrate, 0.5 g; $MgSO_4 \cdot 7H_2O$, 0.1 g; yeast extract, 2.0 g, pH 7.2) was used as growth medium base [40]. As appropriate, bacteria were grown anaerobically in an anaerobic chamber (COY Laboratory Products Inc., Grass Lake, MI, USA) containing 5% hydrogen and 95% nitrogen at 30°C in MMYPF, i.e., MMY supplemented with 75 mM pyruvate (as electron donor) and 44 mM fumarate (as electron acceptor) [40]. In this study, various other media containing different electron donors and acceptors were used as follows: MMYPT (MMY supplemented with 75 mM pyruvate and 2 mM TCE), MMYPN (MMY supplemented with 75 mM pyruvate and 50 mM $NaNO_3$), MMYPD (MMY supplemented with 75 mM pyruvate and 30 mM DMSO), MMYVF (MMY supplemented with 20 mM vanillate and 44 mM fumarate). MMYP refers to MMY base medium supplemented with 75 mM pyruvate. MMYF refers to MMY base medium supplemented with 44 mM fumarate.

### GC–MS analyses

Culture samples (200 µl) were collected and acidified to pH 2 with hydrochloric acid. The metabolites were extracted with 300 µl of ethyl acetate, dried in vacuo, and subsequently trimethylsilylated with TMSI-H (GL Sciences Co., Tokyo, Japan). The resulting sample was subjected to gas chromatography–mass spectrometry (GC–MS) analysis (QP2010 plus, Shimadzu, Kyoto, Japan) with a DB-5 column (30 m in length and 0.25 mm in diameter; J&W Scientific Inc.). The column temperature was first kept at 50°C for 5 min before being increased to 250°C at a rate of 2.5°C/min. The injection and detection temperatures were 250 and 300°C, respectively.

### HPLC analyses

Samples were centrifuged (10,000×*g*, 10 min, 4°C), and the resulting supernatants were subjected to high-performance liquid chromatography (HPLC) analysis using standard protocols as per the manufacturer's instructions. The concentrations of pyruvate, fumarate, acetate, succinate, and DMSO were determined using an 8020 apparatus (Tosoh Co., Tokyo, Japan) equipped with an electric conductivity detector and a TSKgel OApak-A column (Tosoh Co.) operating at 40°C with a 0.75 mM $H_2SO_4$ mobile phase at a flow rate of 1.0 ml/min.

### Nitrate and nitrite assays

Culture samples were centrifuged at 10,000×*g* for 10 min at 4°C to remove cells; the resulting supernatants were subsequently assayed. Nitrate and nitrite concentrations were determined by a modified Griess method as previously reported [31] using an $NO_2/NO_3$ assay Kit-CII (Dojindo Co., Kumamoto, Japan).

### Nucleic acid manipulations

Cells used in this study for total RNA isolation were collected from exponential phase cultures. Y51 cells were harvested by centrifugation (10,000×*g*, 10 min, 4°C). RNA stabilization and mechanical disruption of the collected cells were performed according to the RNAprotect™ bacteria reagent handbook (Qiagen, Inc. Germany). RNeasy Mini Kit (Qiagen) was used to isolate RNA; contaminating DNA was digested using an RNase-Free DNase Set (Qiagen). The RNA samples thus obtained were concentrated to approximately 10 μg/μl using a Microcon YM-30 column (Millipore Co., USA). RNA concentrations were measured at 260 nm with a spectrophotometer. A CyScribe Post-Labelling Kit (Amersham Pharmacia) was used to synthesize cDNAs using random hexamers as primers, and Cy3 or Cy5 dye as labeling agent. A total of 40 μg of total RNA was used for each preparation. The labeled probe thus generated was purified using a CyScribe GFX Purification Kit (Amersham Pharmacia). All procedures were performed as per the manufacturers' instructions.

### Microarray preparation

Oligomer (60-mer) probes for the entire set of the coding sequences of strain Y51 (5,060 sequences; accession number AP008230) were designed, synthesized, and spotted on a Takara-Hubble slide glass by Takara Bio Inc (Kyoto, Japan). Notably, the design of each probe was verified using a BLAST search against the genome of strain Y51 to ensure specificity. As negative controls, 60-mer signature sequences of a number of heterologous dehalogenase genes were spotted on the same microarray; all these control genes were selected from the genomes of halorespiring bacteria such as *D. hafniense* TCE1, *Desulfitobacterium* sp. PCE-S, *Dehalococcoides* sp. FL2, *Dehalococcoides* sp. BAV1, and *Desulfitobacterium dehalogenase*. Moreover, PCE and TCE dehalogenases as well as putative trigger factors also were included [6].

### Microarray hybridization and data analysis

The microarray slides were washed three times using 2× SSC (1× SSC is defined as follows: 0.15 M NaCl, 0.015 M sodium citrate) containing 0.2% SDS and used immediately for hybridization in a Lucidea SlidePro system (Amersham Biosciences). Labeled cDNAs (100 μl) were mixed with an equal volume of hybridization buffer (12× SSC, 0.4% SDS, 10× Denhardt's solution, 0.2 mg/ml denatured salmon sperm DNA in water). Hybridizations were performed at 60°C for 14 h. After hybridization, the slides were washed once with 2× SSC containing 0.2% SDS for 6 min at 35°C, and once with 0.2× SSC containing 0.2% SDS for 6 min at 35°C. The slides were subsequently washed three times using 0.2× SSC, rinsed with isopropanol twice, and dried by airing.

The slides were scanned for Cy3 and Cy5 fluorescent signals with a scanner (FLA-800, Fujifilm, Japan). Image processing and normalization were carried out using GenePix Pro5.1 (Axon Instruments). Median intensities were used in this study; this is often a preferred method as compared with arithmetic mean intensities since median intensity values are less susceptible to the impact of extreme values at either end of a distribution. The median ratio is the ratio of the value of the background from which the median pixel intensity at the second wavelength has been subtracted to the value of the background from which the median pixel intensity at the first wavelength has been subtracted. The average ratio of medians was normalized to 1.0. GeneSpring version 7.3 (Silicon Genetics) was used for statistical analysis. Each pair was compared in the Student's *t* test using GeneSpring; *P* values of the data included in the study and calculated with the Student's *t* test algorithm based on the differences between the ratio values of medians for three biological cultures with duplicate were all lower than 0.05, indicating that measured differences between two conditions were significant at the 95% confidence level.

### Real-time PCR

The real-time (RT)-PCR approach implemented here is a standard method in a 96-well format using a 7500 Fast

Real-Time PCR system (Applied Biosystems, Warrington, UK). This experiment required three separate setups (namely, samples from MMYPF cultures vs. MMYVF; MMYPT vs. MMYPN, and MMYPF vs. MMYPD) in which two different samples were tested for each setup. Reactions contained 10 µl SYBR Green PCR Master Mix (2× , Applied Biosystems), 0.1 µl reverse transcriptase, 0.8 µl RNA (4 ng/µl), and 1 µl of each forward and reverse primer in a total volume of 20 µl. The thermal profile used for amplification was initiated by incubating at 50°C for 30 min and 95°C for 10 min followed by 40 cycles of 95°C for 15 s and 60°C for 1 min. At the end of the amplification phase, a melting curve analysis was carried out on the products formed. All primers were designed by Primer Express 3.0 (Applied Biosystems). RT-PCR data were analyzed using the comparative threshold cycle method as described in a user bulletin from Applied Biosystems. The RNA polymerase beta subunit gene encoded by DSY0464 was chosen as a housekeeper reporter gene, because it is essentially expressed at the same level in all media.

## Results and discussion

### Growth of strain Y51 strain in the presence of various electron donor/acceptor pairs

The growth of strain Y51 in MMYP medium containing PCE or TCE as terminal electron acceptor and the identification of intermediates of PCE and TCE degradation have been reported in previous studies [6, 40]. Strain Y51 was reported to grow in MMY medium to an optical density at 660 nm of 0.9 in 24 h when pyruvate is used as a carbon source and electron donor, with the cell density significantly increasing upon the addition of 44 mM fumarate as an electron acceptor [40]. Lactate also supports the growth of this strain; however, formate only supports significantly slower growth than pyruvate or lactate, whereas succinate, citrate, malate, acetate, glutamate, alanine, methanol, ethanol, glucose, fructose, lactose, or maltose do not support growth at all [28, 40]. It is also worth noting that *D. hafniense* Y51 cells grow in the presence of nitrate or sulfate when pyruvate is the electron donor; however, only poor growth is attained with pyruvate and nitrite or sulfite [40]. Building on these data, we revisited the range of electron donors and acceptors that sustain the growth of strain Y51 (Fig. 1). For example, we observed that strain Y51 grows slowly in MMYVF medium, which contained 20 mM vanillate and 44 mM fumarate (data not shown). This may be ascribed to the absence of an efficient vanillate transport system in *D. hafniense* cells, since no specific vanillate transport system could be found in the strain Y51 genome. Nevertheless, vanillate was converted to protocatechuate as determined by GC–MS analysis and mass spectrometry. Notably, major fragment ions at *m*/*z* of 370, 355, 311, 281, 267, and 193 were observed that indicate the presence of an *O*-demethylation system involved in the metabolism of vanillate [5, 26]. This merits further study since vanillate is one of the phenyl methyl ethers of lignin, thus abundant in forest soil, and since dehalorespiring bacteria have been reported to catabolize these compounds under anoxic conditions and to utilize them as energy sources [5, 12, 26]. Furthermore, the observation that *D. hafniense* is apparently only capable of nitrate respiration but not of nitrite respiration also is worth noting since four nitrite reductase gene homologs (DSY2471-2472 and DSY3065-3066) are present in the genome of strain Y51.

The outcome of these simple growth and metabolite detection analyses was a confirmation that strain Y51 is equipped with apparatuses that support several modes of respiration, with fumarate being completely reduced to succinate, DMSO completely consumed after 38 h, and nitrate reduced to nitrite. To understand the molecular events and regulation of gene expression that take place under these different environmental conditions, and to identify the set of genes involved in these respirations, we compared the transcriptomes of cells grown under these various electron donor and acceptor pairs by microarray analysis, as follows. Emphasis was placed on detecting important genes that are either regulated by a factor of twofold (measured using DNA arrays and summarized in the tables) or constitutively expressed in significant amounts (measured by quantitative PCR and reported in the text as necessary).

### Pyruvate oxidation

Total RNA isolated from MMYPF and MMYVF cultures were reverse-transcribed to cDNAs and labeled with Cy3 and Cy5 dyes. Changes in expression levels were measured as the ratio of Cy3 to Cy5 signals as described in the "Materials and methods" section. Genes likely involved in pyruvate or vanillate metabolisms and that were either up- or downregulated more than twofold as a cutoff level are shown in Table 1. In halorespiring bacteria, it has been reported that pyruvate is converted to acetyl-CoA and formate by PFL [9, 16]. When PCE is present, the electrons for PCE reduction are transferred through a series of reactions catalyzed by FHL and hydrogenase. Although on the genome of strain Y51 there are many coding sequences (CDSs) that have been annotated as putative genes encoding PFL (DSY0416-0417, DSY1551, DSY3009, DSY3016, DSY5006), FHL (DSY2474-2477, DSY2758, DSY3098-3099, DSY3114-3119, DSY3228, DSY4179, DSY4290, DSY5043-5044), and hydrogenase (DSY0794-0796, DSY1596-1599, DSY2100-2101, DSY2238-2240,

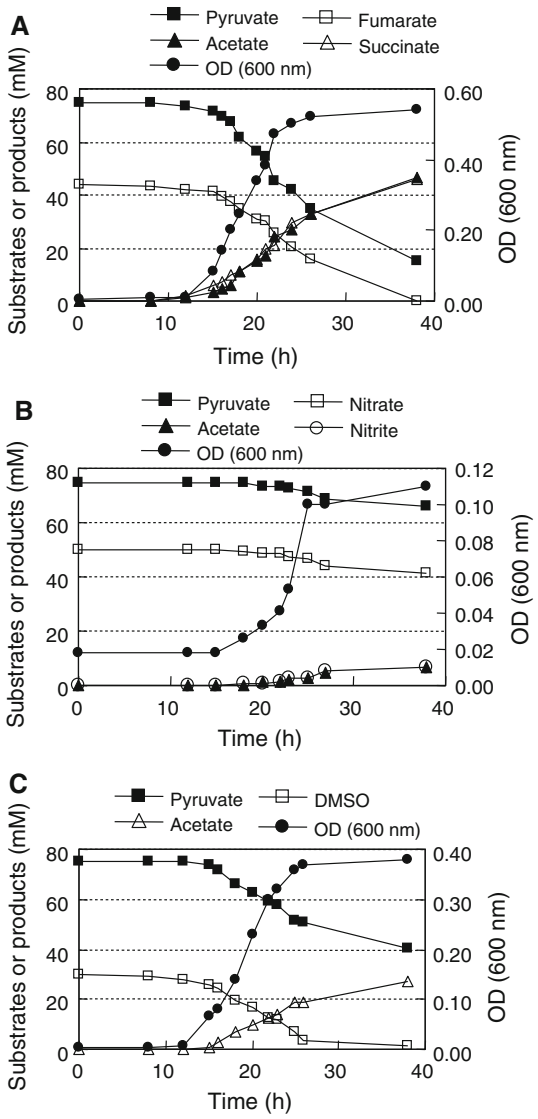


**Fig. 1** Growth of *D. hafniense* strain Y51 in media containing various electron donors and acceptors. Strain Y51 was grown in MMYPF (MMY with pyruvate and fumarate) (**a**), MMYPN (MMY with pyruvate and nitrate) (**b**), and MMYPD (MMY with pyruvate and DMSO) (**c**). The concentrations of electron donors, electron acceptors, and their metabolites are represented. The reported data represent averages calculated from three independent experiments each performed in duplicate. Standard deviations were less than 5%. The concentration of each compound was determined by HPLC analysis using purchased compounds as standards, and the respective retention times of pyruvate, fumarate, succinate, and DMSO were 18.8, 40.1, 27.1, 30.3, and 22.4 min, respectively

DSY4710) [28], we did not detect on the microarray slides any outstanding signal for these genes, suggesting that their expression levels under the conditions tested were very low. As previously mentioned, unlike what is observed in other halorespiring bacteria, formate or $H_2$ as electron donor support only very poor growth of strain Y51 if at all [28, 40].

Taken together, these results promote the view that the electron flow from pyruvate to various electron acceptors does not proceed via formate and $H_2$ in strain Y51 (Fig. 2). Nevertheless, additional work beyond the scope of this paper would be needed to confirm or discard this working hypothesis, including using other electron donors for growth or carbon sources.

Under anaerobic conditions, pyruvate-ferredoxin oxidoreductase (POR) has been shown to play a key role in the oxidative decarboxylation of pyruvate to acetyl-CoA [4, 11, 29]. POR is a thiamine pyrophosphate (TPP)-containing iron–sulfur protein that uses ferredoxin (Fd), or alternatively flavodoxin, as electron acceptor. The low redox potential electrons released during the TPP-based catalytic reaction have to be transferred from a two-electron-donating substrate, pyruvate, to Fd. Strain Y51 harbors two CDSs coding for POR, namely, DSY0115 and DSY4888 (Fig. 2). Whereas no detectable signal was obtained for DSY4888, DSY0115 appeared to be upregulated 6.9-fold in pyruvate-containing medium as opposed to vanillate-containing medium (Table 1). This suggests that the product of this gene may play a crucial role in the conversion of pyruvate to acetyl-CoA. To verify the validity and the accuracy of this microarray analysis experiment, several genes, including DSY0115, were selected for RT-PCR analysis. The data obtained by RT-PCR were in general in good agreement with those obtained by microarray analysis. For example, DSY0115 was measured by RT-PCR to be upregulated 6.2-fold.

POR genes have been isolated from a variety of anaerobic bacteria, archaea, and eukaryotes; three types of POR can be distinguished on the basis of molecular structures. DSY0115 belongs to the group of POR that contains four different subunits per molecule and constitutes a homodimeric enzyme. The crystal structure of this group of proteins was reported for *Desulfovibrio africanus* [4]. DSY0115 exhibits 69% similarity at the amino acid level with the POR of *D. africanus*. Three distinct Fds named Fd I, Fd II, and Fd III have been isolated from *D. africanus* [29, 30]. Similarly, three Fd families were found on the genome of strain Y51: two Fd I, nine Fd II, and three Fd III. Remarkably, only one of these, Fd I (DSY1451), was strongly expressed and upregulated by 2.2-fold in MMYPF medium (Table 1). This result suggests that DSY1451 plays a critical role in this respiration. It is also worth noting that no CDS similar to Fd-NAD(P)$^+$ reductase genes was found in the genome of strain Y51; these enzymes have been reported in many anaerobic bacteria to transfer electrons from Fd to the low potential electron acceptor, NAD(P)H [3].

It has been proposed that, in strain Y51, pyruvate is ultimately converted into acetate through acetyl-CoA. A possible pathway for this conversion was identified in the

**Table 1** Gene expression ratios comparing MMYPF and MMYVF

| CDS ID | Predicted function | Expression ratio | Signal intensity | |
|---|---|---|---|---|
| | | | MMYVF | MMYPF |
| DSY0115 | Pyruvate:ferredoxin oxidoreductase (POR) | 6.9 | 89 | 607 |
| DSY0138 | 5,10-Methylenetetrahydrofolate reductase | 0.16 | 509 | 82 |
| DSY0205 | Formyltetrahydrofolate synthetase | 0.16 | 660 | 100 |
| DSY0308 | Ferredoxin III | 0.04 | 371 | 17 |
| DSY0605 | Formyltetrahydrofolate synthetase | 0.01 | 151 | −1[b] |
| DSY0606 | Methenyl tetrahydrofolate cyclohydrolase | 0.01 | 129 | −1.2[b] |
| DSY0607 | 5,10-Methylenetetrahydrofolate dehydrogenase | 0.01 | 419 | −0.67[b] |
| DSY1451 | Ferredoxin I | 2.2 | 2,487 | 4,974 |
| DSY1596 | Ni,Fe-hydrogenase maturation factor | 0.10 | 1,091 | 115 |
| DSY1597 | Ni,Fe-hydrogenase I cytochrome $\beta$ subunit | 0.03 | 5,851 | 151 |
| DSY1598 | Ni,Fe-hydrogenase I large subunit | 0.02 | 575 | 13 |
| DSY1599 | Ni,Fe-hydrogenase I small subunit | 0.06 | 2,702 | 184 |
| DSY1647 | N5-Methyltetrahydromethanopterin methyltransferase | 0.02 | 181 | 2 |
| DSY1648 | CO dehydrogenase/acetyl-CoA synthase delta subunit | 0.01 | 2,214 | 31 |
| DSY1649 | CO dehydrogenase maturation factor | 0.01 | 124 | −1.5[b] |
| DSY1650 | Ferredoxin | 0.01 | 960 | 6.6 |
| DSY1651 | CO dehydrogenase/acetyl-CoA synthase gamma subunit | 0.01 | 103 | −2.7[b] |
| DSY1652 | CO dehydrogenase/acetyl-CoA synthase beta subunit | 0.01 | 163 | −0.20[b] |
| DSY1653 | 6Fe–6S prismane cluster-containing protein | 0.01 | 1,552 | 12 |
| DSY1654 | CO dehydrogenase maturation factor | 0.02 | 530 | 11 |
| DSY2355 | Methenyl tetrahydrofolate cyclohydrolase | 0.34 | 31 | 11 |
| DSY2356 | 5,10-Methylenetetrahydrofolate dehydrogenase | 0.29 | 116 | 34 |
| DSY2400 | Phosphotransacetylase | 0.02 | 50 | 1.3 |
| DSY2401 | Acetate kinase | 0.60 | 20 | 12 |
| DSY2668 | Acetate kinase | 5.9 | 46 | 270 |
| DSY3155 | Corrinoid protein | 0.01 | 6,394 | 11 |
| DSY3156 | Phenyl methylether:corrinoid protein methyl transferase | 0.01 | 283 | −1.8[b] |
| DSY3157 | Methylcorrinoid protein:tetrahydrofolate methyl transferase | 0.01 | 396 | −1[b] |
| DSY3968 | Formate dehydrogenase, typically selenocysteine-containing | 0.12 | 1,516 | 182 |
| DSY3969 | Formate dehydrogenase | 0.13 | 199 | 26 |
| DSY3970 | Formate dehydrogenase | 0.17 | 679 | 117 |
| DSY3972 | 5-Formyltetrahydrofolate cyclo-ligase | 0.36 | 725 | 253 |
| DSY4199 | Phenyl methylether:corrinoid protein methyl transferase | 2.1 | 404 | 915 |
| DSY4888 | Pyruvate:ferredoxin oxidoreductase (POR) | ND[a] | ND | ND |

*MMYPF* MMY supplemented with pyruvate and fumarate, *MMYVF* MMY supplemented with vanillate and fumarate

[a] ND, signal was not detected

[b] Values lower than or equal to 0 were set to 0.01 by the GeneSpring analysis software

genome of this strain [28], which contains a phosphotransacetylase encoded by DSY2400 and acetate kinases encoded by DSY2668 and DSY2401. Interestingly, only the acetate kinase encoded by DSY2668 was expressed in MMYPF medium (Table 1). However, this does not exclude the possibility that heretofore unidentified gene products are involved in this conversion.

## PCE dehalogenase

We compared the levels of gene expression in cells grown in either MMYPT (with TCE as electron acceptor) or MMYPN (with nitrate as electron acceptor) as a means to identify the genes responsible for both PCE and nitrate respiration with the view that under industrial field

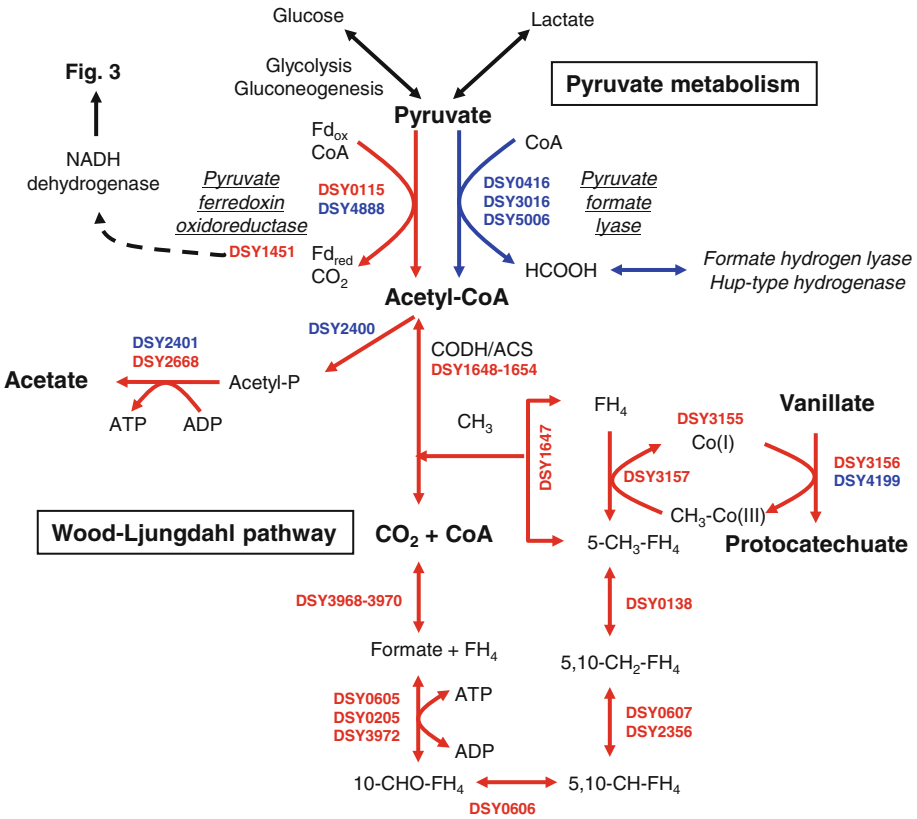


**Fig. 2** Proposed metabolic pathways for pyruvate and vanillate. Genes represented in *red* were induced by pyruvate or vanillate (upregulated), genes represented in *blue* were not expressed in pyruvate- or vanillate-containing media. Detailed information is provided in the text. *D. hafniense* is not known to be autotrophic and the role of the Wood–Ljungdahl pathway, which is strongly induced by vanillate, remains unclear in this organism. One of the functions of the pathway could be to channel methyl groups from phenyl methyl ethers, such as vanillate, to the central metabolism. Co(I), corrinoid protein; $CH_3$–Co(III), methylcorrinoid protein; $Fd_{ox}$, oxidized ferredoxin; $Fd_{red}$, reduced ferredoxin. Compounds: $FH_4$, tetrahydrofolate; 5-$CH_3$-$FH_4$, 5-methyl-$FH_4$; 5,10-$CH_2$-$FH_4$, 5,10-methylene-$FH_4$; 5,10-CH-$FH_4$, 5,10-methenyl-$FH_4$; 10-CHO-$FH_4$, 10-formyl-$FH_4$

bioremediation conditions, dehalorespiration rather than nitrate respiration is to be promoted. TCE was used instead of PCE in our laboratory model because TCE supports better than PCE the growth of strain Y51. This is appropriate at this stage since, as previously reported, PCE and TCE dehalogenation are catalyzed by the same enzyme system in this strain [6, 40, 41]. Genes responsible for PCE and nitrate catabolism, and that were either up- or down-regulated more than twofold, are reported in Table 2. Surprisingly, transcription of the genes *pceA* and *pceB* coding for the tetrachloroethene dehalogenase structural protein and its putative membrane anchor protein were not upregulated in TCE-containing medium (Tables 1, 2, 3, 4). What is more, the entire gene cluster *pceABCT* was expressed at high levels also in the other media used in this study, thus suggesting that the *pceABCT* genes that form an operon, with *pceABC* being transcribed in a polycistronic manner and *pceT* being primarily transcribed in a monocistronic manner [8, 22, 28], are constitutively expressed. These data confirm observations reported elsewhere in the presence of chloromethanes [8]. Nevertheless, *pceT* coding for the trigger factor protein PceT involved in folding of the PceA precursor and *pceC* coding for a putative transcriptional regulator of the NirI/NosR family [22] seem subject to regulatory control (Tables 2, 3), since during TCE respiration, *pceT* is induced twofold whereas *pceC* is downregulated twofold (Table 2). On the other hand, no significant changes in the mRNA levels of *pceA* have been measured in *D. hafniense* Y51 in any of the four different media tested, a result confirmed by RT-PCR data, similarly to what was observed in *D. hafniense* TCE1 in TCE-containing medium 717 [32]. Nevertheless, proteomics experiments demonstrated in strain TCE1 that the reductive dehalogenase PceA is highly regulated since its level is 70- to 100-fold higher when cells are grown in the presence of PCE as compared with fumarate [32].

Remarkably, the transcription of the transposases of the two insertion sequences of the IS*Desp* elements (DSY2834 and DSY2840) that flank the *pceABCT* genes increases by approximately 50–60% in *D. hafniense* Y51 cells incubated

**Table 2** Gene expression ratios comparing MMYPT with MMYPN

| CDS ID | Predicted function | Expression ratio | Signal intensity | |
|---|---|---|---|---|
| | | | MMYPN | MMYPT |
| DSY0185 | Uncharacterized component of anaerobic dehydrogenase | 5.4 | 181 | 922 |
| DSY0188 | DMSO reductase anchor subunit | 11 | 28 | 285 |
| DSY0291 | ABC-type cobalamin/$Fe^{3+}$ transport system, periplasmic component | 3.2 | 38 | 115 |
| DSY0317 | Sulfite reductase, gamma subunit | 29 | 11 | 333 |
| DSY0318 | Cobyrinic acid *a*,*c*-diamide synthase | 5.2 | 13 | 68 |
| DSY0332 | Nitrate/nitrite transporter | 0.01 | 594 | 6 |
| DSY0333 | Nitrate/nitrite transporter | 0.01 | 57 | −0.67[a] |
| DSY0334 | Anaerobic dehydrogenases, typically selenocysteine-containing (NarG) | 0.03 | 36 | 0.37 |
| DSY0335 | Nitrate reductase beta chain (NarH) | 0.12 | 32 | 3.6 |
| DSY0336 | Nitrate reductase delta subunit (NarJ) | 0.08 | 58 | 6.5 |
| DSY0337 | Nitrate reductase gamma subunit (NarI) | 0.13 | 77 | 8 |
| DSY0715 | Ferredoxin II | 0.11 | 214 | 22 |
| DSY0733 | Flavodoxin | 2.3 | 304 | 727 |
| DSY1155 | Chlorophenol reductive dehalogenase | 225 | 25 | 5,570 |
| DSY1451 | Ferredoxin I | 4.0 | 2,233 | 8,832 |
| DSY1479 | Cobalamin biosynthesis protein CbiM | 2.0 | 48 | 99 |
| DSY1480 | ABC-type cobalt transport system, periplasmic component | 2.2 | 179 | 391 |
| DSY1626 | Ferredoxin-like protein | 8.1 | 52 | 413 |
| DSY1629 | Electron transfer flavoprotein beta subunit | 4.1 | 40 | 168 |
| DSY1764 | ABC-type cobalamin/$Fe^{3+}$ transport system, periplasmic component | 5.1 | 36 | 185 |
| DSY2231 | Fe–S-cluster-containing hydrogenase components 1 | 5.4 | 80 | 404 |
| DSY2471 | Nitrate/trimethylamine N-oxide (TMAO) reductases, membrane-bound tetraheme cytochrome *c* subunit (NrfH) | ND[b] | ND | ND |
| DSY2472 | Formate-dependent nitrite reductase, periplasmic cytochrome *c552* subunit (NrfA) | ND | ND | ND |
| DSY2834 | Predicted transposase (TnpA1) | 1.5 | 266 | 381 |
| DSY2836 | Putative trigger factor (PceT) | 2.1 | 1,547 | 3,039 |
| DSY2837 | Putative transcriptional regulator (PceC) | 0.52 | 537 | 291 |
| DSY2838 | Putative membrane anchor protein (PceB) | 1.2 | 5,516 | 6,340 |
| DSY2839 | PCE dehalogenase (PceA) | 1.0 | 1,899 | 1,909 |
| DSY2840 | Predicted transposase (TnpA2) | 1.6 | 246 | 417 |
| DSY3065 | Formate-dependent nitrite reductase, periplasmic cytochrome *c552* subunit (NrfA) | 3.7 | 198 | 753 |
| DSY3066 | Nitrate/TMAO reductase, membrane-bound tetraheme cytochrome *c* subunit (NrfH) | 3.1 | 216 | 660 |
| DSY3087 | Fe–S oxidoreductase | 3.0 | 261 | 784 |
| DSY3139 | Fumarate reductase, flavoprotein subunit (FrdA) | 14 | 89 | 1,270 |
| DSY3309 | Predicted Fe–S oxidoreductase | 2.4 | 44 | 104 |
| DSY4014 | Anaerobic dehydrogenases, typically selenocysteine-containing | 2.5 | 197 | 491 |
| DSY4055 | Cytochrome *bd*-type quinol oxidase, subunit 2 | 1.3 | 90 | 124 |
| DSY4056 | Cytochrome *bd*-type quinol oxidase, subunit 1 | 2.9 | 260 | 810 |
| DSY4463 | Thioredoxin reductase | 27 | 10 | 273 |
| DSY4471 | Thioredoxin reductase | 4.6 | 111 | 528 |

*MMYPT* MMY supplemented with pyruvate and TCE, *MMYPN* MMY supplemented with pyruvate and nitrate

[a] ND, signal was not detected

[b] Values lower than or equal to 0 were set to 0.01 by the GeneSpring analysis software

in the presence of pyruvate/TCE, as compared with cells incubated in the presence of pyruvate/nitrate (Table 2). Together with the observation that the RecA protein is 19-fold more abundant in strain TCE1 cells incubated in the presence of hydrogen/PCE as compared with hydrogen/fumarate [32], this observation suggests a possible stress

**Table 3** Gene expression ratios comparing MMYPF with MMYPN

| CDS ID | Predicted function | Expression ratio | Signal intensity | |
|---|---|---|---|---|
| | | | MMYPN | MMYPF |
| DSY0332 | Nitrate/nitrite transporter | 0.01 | 782 | 2.0 |
| DSY0333 | Nitrate/nitrite transporter | 0.01 | 43 | 0[a] |
| DSY0334 | Anaerobic dehydrogenase, typically selenocysteine-containing (NarG) | 0.01 | 90 | 0[a] |
| DSY0335 | Nitrate reductase beta chain (NarH) | 0.03 | 24 | 1.0 |
| DSY0336 | Nitrate reductase delta subunit (NarJ) | 0.04 | 62 | 2.3 |
| DSY0337 | Nitrate reductase gamma subunit (NarI) | 0.03 | 148 | 4.5 |
| DSY0715 | Ferredoxin II | 0.06 | 273 | 16 |
| DSY0735 | Fumarate reductase cytochrome *b* subunit (FrdC) | ND | ND | ND |
| DSY0736 | Fumarate reductase, flavoprotein subunit (FrdA) | ND | ND | ND |
| DSY0737 | Fumarate reductase, Fe–S protein (FrdB) | ND | ND | ND |
| DSY1155 | Chlorophenol reductive dehalogenase | 95 | 22 | 2,118 |
| DSY1353 | ABC-type nitrate/sulfonate/taurine/bicarbonate transport system, ATPase component | 0.01 | 228 | 2.5 |
| DSY1354 | ABC-type nitrate/sulfonate/taurine/bicarbonate transport system, periplasmic component | 0.01 | 161 | 1.0 |
| DSY1355 | ABC-type nitrate/sulfonate/taurine/bicarbonate transport system, permease component | 0.02 | 258 | 3.7 |
| DSY1451 | Ferredoxin I | 2.5 | 1,984 | 4,832 |
| DSY2471 | Nitrate/TMAO reductase, membrane-bound tetraheme cytochrome *c* subunit (NrfH) | ND[b] | ND | ND |
| DSY2472 | Formate-dependent nitrite reductase, periplasmic cytochrome *c552* subunit (NrfA) | ND | ND | ND |
| DSY2834 | Predicted transposase (TnpA1) | 1.5 | 221 | 327 |
| DSY2836 | Putative trigger factor (PceT) | 2.5 | 966 | 2,174 |
| DSY2837 | Putative transcriptional regulator (PceC) | 1.1 | 691 | 739 |
| DSY2838 | Putative membrane anchor protein (PceB) | 1.1 | 5,254 | 5,611 |
| DSY2839 | PCE dehalogenase (PceA) | 1.3 | 1,496 | 1,861 |
| DSY2840 | Predicted transposase (TnpA2) | 1.3 | 289 | 370 |
| DSY3065 | Formate-dependent nitrite reductase, periplasmic cytochrome *c552* subunit (NrfA) | 0.77 | 151 | 113 |
| DSY3066 | Nitrate/TMAO reductase, membrane-bound tetraheme cytochrome *c* subunit (NrfH) | 0.69 | 234 | 159 |
| DSY3139 | Fumarate reductase, flavoprotein subunit (FrdA) | 8.4 | 62 | 464 |
| DSY4006 | ABC-type nitrate/sulfonate/taurine/bicarbonate transport system, ATPase component | 0.12 | 190 | 22 |
| DSY4007 | ABC-type nitrate/sulfonate/taurine/bicarbonate transport system, permease component | 0.08 | 1,433 | 107 |
| DSY4008 | ABC-type nitrate/sulfonate/taurine/bicarbonate transport system, periplasmic component | 0.14 | 377 | 51 |
| DSY4055 | Cytochrome *bd*-type quinol oxidase, subunit 2 | 2.5 | 194 | 482 |
| DSY4056 | Cytochrome *bd*-type quinol oxidase, subunit 1 | 2.1 | 428 | 883 |

*MMYPF* MMY supplemented with pyruvate and fumarate, *MMYPN* MMY supplemented with pyruvate and nitrate

[a] Values lower than or equal to 0 were set to 0.01 by the GeneSpring analysis software

[b] ND, signal was not detected

response during dechlorination and poses the question whether the *pceABCT* gene dosage could increase during PCE challenge. Noteworthily, the emergence of nondechlorinating variants of strain Y51 has been observed in serial subcultures in PCE-free media revealing the instability of the *pceABCT* cluster [7].

By comparing with other terminal respiration systems [1, 13, 42, 45], it was expected that in addition to PceABCT proteins, at least a cytochrome *b* and an electron transport protein (Fe–S protein) are required for PCE respiration. A list of the CDSs that have been annotated to encode cytochrome *b* or Fe–S proteins, and that were upregulated in TCE-containing medium, is shown in Table 2. These include DSY4055-4056, which encode a cytochrome *bd*-type quinol oxidase, DSY1451, which encodes a ferredoxin, and DSY1626, DSY1629, DSY0733, and DSY3309, which encode four different Fe–S proteins. Further studies are required to determine whether these are involved in PCE and TCE respiration.

In addition to PceA (DSY2839), strain Y51 exhibits another dehalogenase (DSY1155), which is very similar to the *ortho*-chlorophenol reductase of *D. frappieri* PCP-1, a polychlorophenol-respiring bacterium [2]. The function of this putative chlorophenol reductive dehalogenase is worth

**Table 4** Gene expression ratios comparing MMYPF with MMYPD

| CDS ID | Predicted function | Expression ratio | Signal intensity | |
|---|---|---|---|---|
| | | | MMYPD | MMYPF |
| DSY0185 | Uncharacterized component of anaerobic dehydrogenase | 0.34 | 581 | 183 |
| DSY0186 | Anaerobic dehydrogenase, typically selenocysteine-containing (DmsA) | 0.11 | 132 | 16 |
| DSY0187 | Fe–S-cluster-containing hydrogenase component (DmsB) | 0.12 | 75 | 9.3 |
| DSY0188 | DMSO reductase anchor subunit (DmsC) | 0.15 | 580 | 90 |
| DSY0596 | Uncharacterized component of anaerobic dehydrogenase | 0.01 | 4,446 | 2.2 |
| DSY0597 | Anaerobic dehydrogenase, typically selenocysteine-containing (DmsA) | 0.01 | 138 | −3.4[a] |
| DSY0598 | Fe–S-cluster-containing hydrogenase component (DmsB) | 0.01 | 413 | −1.2[a] |
| DSY0599 | DMSO reductase anchor subunit (DmsC) | 0.01 | 1,229 | −1.4[a] |
| DSY1647 | Methylcorrinoid protein:tetrahydrofolate methyl transferase | 0.01 | 326 | 2.2 |
| DSY1648 | CO dehydrogenase/acetyl-CoA synthase delta subunit | 0.01 | 978 | 11 |
| DSY1649 | CO dehydrogenase maturation factor | 0.01 | 287 | 0.50 |
| DSY1650 | Ferredoxin | 0.01 | 442 | 3.0 |
| DSY1651 | CO dehydrogenase/acetyl-CoA synthase gamma subunit | 0.01 | 428 | 2.5 |
| DSY1652 | CO dehydrogenase/acetyl-CoA synthase beta subunit | 0.01 | 1,058 | 0.83 |
| DSY1653 | 6Fe–6S prismane cluster-containing protein | 0.02 | 523 | 5.7 |
| DSY1654 | CO dehydrogenase maturation factor | 0.02 | 300 | 5.8 |
| DSY3139 | Fumarate reductase, flavoprotein subunit (FrdA) | 0.51 | 1,486 | 707 |
| DSY3155 | Corrinoid protein | 1.0 | 21 | 22 |
| DSY3408 | Uncharacterized component of anaerobic dehydrogenase | 0.20 | 134 | 26 |
| DSY3409 | DMSO reductase anchor subunit (DmsC) | 0.21 | 165 | 35 |
| DSY3410 | Fe–S-cluster-containing hydrogenase component (DmsB) | 0.12 | 144 | 17 |
| DSY3411 | Anaerobic dehydrogenase, typically selenocysteine-containing (DmsA) | 0.34 | 208 | 71 |
| DSY4199 | Phenyl methylether:corrinoid protein methyl transferase | 1.4 | 236 | 327 |

*MMYPF* MMY supplemented with pyruvate and fumarate, *MMYPD* MMY supplemented with pyruvate and DMSO

[a] Values lower than or equal to 0 were set to 0.01 by the GeneSpring analysis software

exploring further, since our microarray analyses indicated that DSY1155 is induced 225-fold in MMYPT medium (Table 2). In spite of this, strain Y51 has been reported to have no ability for dehalogenating *o*-, *m*-, and *p*-chlorobenzoates [40]. DSY1155 neither occurs in a cluster nor is it surrounded by genes coding for transposases. DSY1155 is not involved in PCE respiration because Y51 strain mutants that lost *pceA* no longer exhibit any PCE dechlorination activity [7, 8]. Moreover, it is currently not known whether strain Y51 dechlorinates polychlorophenols. Notably, in contrast to strain Y51, *D. ethenogenes* strain 195 contains 17 dehalogenase CDSs, four PCE dehalogenase genes, and a periplasmic Ni–Fe hydrogenase gene that exhibited the highest overall expression levels in PCE-fed cultures [23, 24, 27, 34].

## Vanillate metabolism

*Desulfitobacterium hafniense* [26], like *Acetobacterium dehalogenans* [5], and *Moorella thermoacetica* [12], has been reported to employ a tetrahydrofolate ($FH_4$)-dependent aromatic *O*-demethylation system, which converts vanillate to protocatechuate and mediates the transfer of the methyl group to $FH_4$. One gene cluster (DSY3155-3157) of the strain Y51 genome encodes a putative $FH_4$-dependent aromatic *O*-demethylation system; we demonstrated here that this cluster is induced when *D. hafniense* is grown in vanillate-containing medium (Table 1). This observation promotes the view that the methyl group from vanillate is ultimately transferred to a CO dehydrogenase (CODH) and acetyl-CoA synthase (ACS) complex (DSY1647-1654) for generating acetyl-CoA to enter the central metabolism (Fig. 2), since these latter genes also are significantly upregulated in the presence of vanillate (Table 1, and DSY1647 RT-PCR data that indicate a 73-fold upregulation). This hypothesis is further promoted by the observation that the transcriptional upregulation reported here is likely to translate into proteomic abundance in light of the observation that the products of genes DSY1651, DSY1653, and DSY1654 are 13-, 42-, and 13-fold, respectively, more abundant in *D. hafniense* TCE1 cells incubated in the presence of $H_2$/PCE

as compared with $H_2$/fumarate [32]. Noteworthily, CODH and ACS form the key enzymatic complex of the Wood–Ljungdahl pathway, which is a pathway of organic carbon fixation from carbon dioxide present in some bacteria and archaea [33]. This pathway appears functional in strain Y51 since in addition to the CODH/ACS-encoding genes (DSY1647-1654), other genes typical of this pathway are strongly induced in vanillate-containing medium (DSY2356, DSY3155-3157, DSY0138, DSY3968-3970, DSY0605-0607, DSY0205, DSY3972) (Fig. 2). Nonetheless, the specific role of the Wood–Ljungdahl pathway in *Desulfitobacterium* still needs to be demonstrated [32]. It has been proposed that the Wood–Ljungdahl pathway is employed by bacteria for the synthesis of acetyl-CoA when phenyl methyl ethers are present in the culture medium. Moreover, another PCE halorespiring bacterium, *D. tiedjei* DCB-1, has the ability to grow autotrophically using hydrogen as the electron donor in bicarbonate-buffered medium; this metabolism involves CODH/ACS activity as detected in grown cells [21, 39].

### Fumarate reductase

Genes involved in fumarate and nitrate respiration were identified by comparing the transcriptome profiles attained from cells that were grown on either MMYPF or MMYPN. The *pceABCT* operon, genes coding for electron transfer proteins, or genes coding for proteins involved in nitrate or nitrite metabolism and that exhibited an up- or downregulation greater than or equal to twofold are shown in Table 3.

Fumarate reductase has been shown to play a key role in the bioenergetic mechanisms of anaerobic cells using fumarate as a terminal electron acceptor [1, 13]. The enzyme is composed of three subunits: a flavoprotein (FrdA), an iron–sulfur protein (FrdB), and a cytochrome *b* (FrdC). The genome of strain Y51 has a cluster (DSY0735-0737) encoding FrdABC. However, this cluster is neither expressed in MMYPF medium nor in any of the other culture media used in this study. Furthermore, it is surprising that strain Y51 has no fewer than 31 FrdA analogs that do not occur as clusters and to which no FrdBC genes are adjacent. Within the course of these studies, we observed that only one FrdA analog, encoded by DSY3139, is significantly expressed and induced 8.4-fold in MMYPF medium as compared with MMPYN (Table 3; RT-PCR indicates a 6.1-fold increase). Interestingly, DSY3139 is also induced in MMYPT medium as compared with MMYPN (Table 2; RT-PCR indicates a 7.9-fold increase). Considering that fumarate has a structure that is somewhat similar to that of PCE (TCE), a striking hypothesis to explore is whether PCE and fumarate respiration could use the same electron transfer system, since Fd (DSY1451) and cytochrome *bd*-type quinol oxidase (DSY4055-4056) were both upregulated in this pyruvate/fumarate vs. pyruvate/nitrate electron-donor/electron-acceptor comparative experiment.

### DMSO reductase

The genes responsible for DMSO respiration were identified by comparing the patterns of gene expression attained from cells grown in MMYPF or MMYPD (Table 4). It is striking that the CDSs that form the largest group of paralogs in the genome of strain Y51 are those that encode DMSO reductases. These enzymes are terminal electron transfer enzymes, which allow bacteria to grow anaerobically on DMSO as the respiratory oxidant [42, 45]. They consist of a molybdoprotein cofactor-containing subunit (DmsA), an electron-transfer subunit (DmsB), and a membrane-spanning anchor subunit (DmsC). In cells grown in MMYPD, three gene clusters were induced thus indicating their probable involvement in DMSO respiration: DSY0185-0188 and DSY3408-3411, and particularly DSY0596-0599 that reached very high transcript levels (Table 4). These three DMSO reductase clusters share the same four structural genes that code for DmsABC and for an uncharacterized protein.

In addition, we observed that the CODH/ACS gene cluster (DSY1647-1654) is not only induced in MMYVF, but also in MMYPD. This suggests that dimethyl sulfide formed from DMSO is further converted into methanethiol in a demethylation reaction whereby the released methyl group may be used by CODH/ACS to synthesize acetyl-CoA with $CO_2$, as has been reported in other bacteria [15].

## Conclusion and perspectives

The electron flow for PCE respiration has been predicted to occur as follows in various PCE-dechlorinating bacteria: formate $\rightarrow H_2 \rightarrow$ proton + electron $\rightarrow$ MQ $\rightarrow\rightarrow$ PCE [12, 35–37, 44]. In our hands, formate and $H_2$ as electron donors for PCE respiration supported only poorly if at all the respiration and growth of strain Y51 [28] suggesting a different electron flow in *D. hafniense* Y51. The putative electron flows to various electron acceptors described in this study are shown in Fig. 3.

Specifically regarding the electron flow when pyruvate is used as an electron donor, we propose as a working model that pyruvate is converted to acetyl-CoA by the POR encoded by DSY0115 (Fig. 3). According to this model, the electrons from pyruvate are transferred to the Fd encoded by DSY1451, and subsequently to NADH via an unknown route. Remarkably, strain Y51 has one NADH dehydrogenase gene cluster (DSY2578-DSY2588;

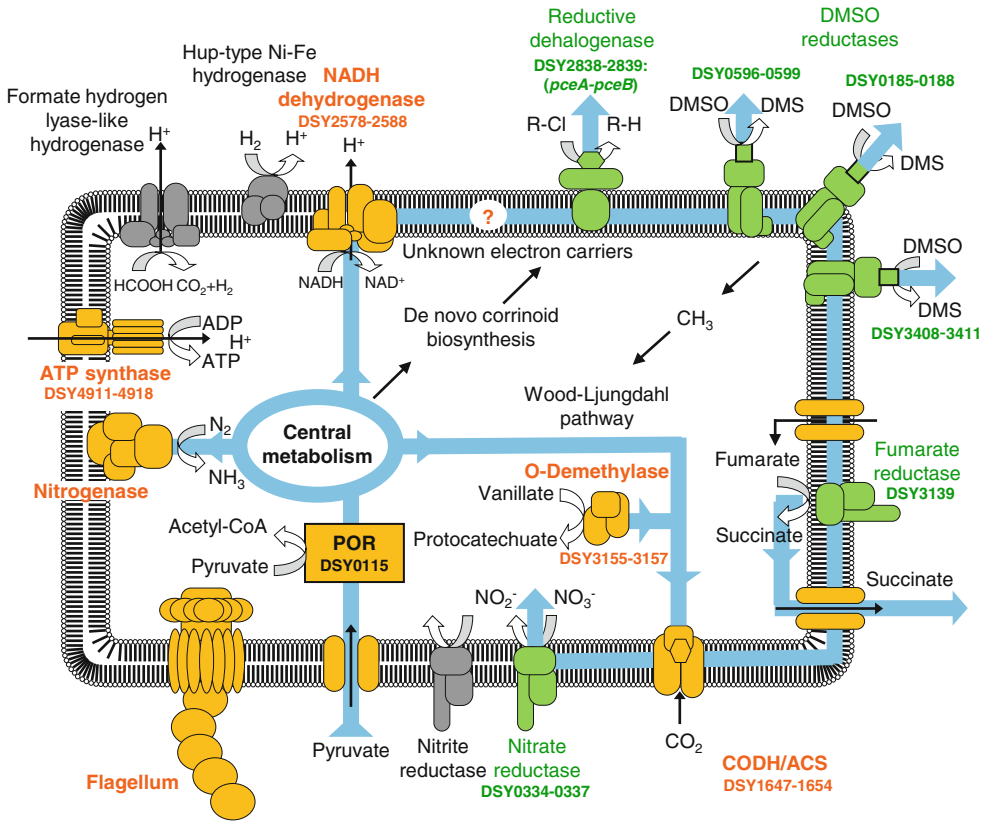


**Fig. 3** Schematic diagram of the metabolic pathway of strain Y51. The proposed electron flow routes are indicated by wide *blue lines*. The reductases that are functional are displayed in *green*. Strain Y51 proteins represented in *gray* did not function under the conditions tested. Notably, high signal intensities were measured in MMYPF for the ATP synthase genes *atpABCDEFGH* (data not shown). The Hup-type Ni–Fe hydrogenase is encoded by DSY0794-0796, DSY1596-1599, DSY2100-2101, DSY2238-2240, and DSY4710; FHL by DSY2474-2477, DSY2758, DSY3098-3099, DSY3114-3119, DSY3228, DSY4179, DSY4290, DSY5043-5044 [28]. *POR* pyruvate:ferredoxin oxidoreductase, *DMSO* dimethyl sulfoxide, *DMS* dimethyl sulfide, *CODH/ACS* CO dehydrogenase/acetyl-CoA synthase. Chlorinated compounds are represented as R-Cl (e.g., PCE or TCE), dechlorinated compounds as R-H (e.g., DCE). The reductive dehalogenase PceA is believed to be anchored into the inner membrane on the periplasmic face by PceB, whereas the trigger factor protein PceT contributes to the correct folding of the PceA precursor for processing by the TAT secretion system and PceC is a putative membrane binding transcriptional regulator [22]. The figure is an adaptation of a diagram published by Nonaka et al. [28]

*nuoNMLKJIHDCBA*), which is constitutively expressed in all culture media used in this study. Although the route of electron transfer from NADH to various reductases remains unclear, it might include several Fe–S proteins. Importantly, the *pceABCT* cluster of strain Y51 appears to be constitutively expressed at a high level, despite being subject to regulation. During lignin degradation initiated by environmental microbial consortia, the Wood–Ljungdahl pathway is apparently used by *D. hafniense* to channel the methyl group from vanillate to the central metabolism via protocatechuate. Nonetheless, this hypothesis would need to be further verified by appropriate physiological experiments.

Strain Y51 exhibits a variety of electron donor and terminal electron acceptor catabolic systems; it can synthesize all its required nucleotides, amino acids, and cofactors, including the complete cobalamin biosynthetic pathway that is involved in the PceA catalytic center [28]. Because there are numerous analogs for each reductase on the genome, analysis of these pathways by microarrays is not sufficient to definitely identify which reductase genes are expressed and at what levels. Nevertheless, transcriptomics data provide an initial view of the very complex physiology of *D. hafniense*. This is important because strain Y51 could potentially be developed into a useful bioremediation agent given its ability to survive in various environmental conditions with or without PCE. Nonetheless, understanding of the instability of the *pceABCT* operon appears to be a prerequisite to the field-scale use of *D. hafniense* Y51. Although this microarray study for the global analysis of the regulation of gene expression in a PCE-dehalorespiring bacterium remains preliminary, it provides the necessary information for formulating research hypotheses for further study, including for the development of a PCE bioremediation activity monitoring device or to engineer a more complete detoxification

pathway, thereby extending the detoxification of PCE/TCE by *D. hafniense* beyond DCE and ideally onto ethene.

**Acknowledgments** We thank Dr. C. Omumasaba (RITE) for critical reading of the manuscript. This research was supported by New Energy and Industrial Technology Development (NEDO), Japan.

## References

1. Biel S, Simon J, Gross R, Ruiz T, Ruitenberg M, Kröger A (2002) Reconstitution of coupled fumarate respiration in liposomes by incorporating the electron transport enzymes isolated from *Wolinella succinogenes*. Eur J Biochem 269:1974–1983
2. Boyer A, Page-Belanger R, Saucier M, Villemur R, Lépine F, Juteau P, Beaudet R (2003) Purification, cloning and sequencing of an enzyme mediating the reductive dechlorination of 2,4,6-trichlorophenol from *Desulfitobacterium frappieri* PCP-1. Biochem J 373:297–303
3. Carrillo N, Ceccarelli EA (2003) Open questions in ferredoxin-$NADP^+$ reductase catalytic mechanism. Eur J Biochem 270: 1900–1915
4. Chabrière E, Vernède X, Guigliarelli B, Charon MH, Hatchikian EC, Fontecilla-Camps JC (2001) Crystal structure of the free radical intermediate of pyruvate:ferredoxin oxidoreductase. Science 294:2559–2563
5. Engelmann T, Kaufmann F, Diekert G (2001) Isolation and characterization of a veratrol:corrinoid protein methyl transferase from *Acetobacterium dehalogenans*. Arch Microbiol 175:376–383
6. Furukawa K, Suyama A, Tsuboi Y, Futagami T, Goto M (2005) Biochemical and molecular characterization of a tetrachloroethene dechlorinating *Desulfitobacterium* sp. strain Y51: a review. J Ind Microbiol Biotechnol 32:534–541
7. Futagami T, Tsuboi Y, Suyama A, Goto M, Furukawa K (2006) Emergence of two types of nondechlorinating variants in the tetrachloroethene-halorespiring *Desulfitobacterium* sp. strain Y51. Appl Microbiol Biotechnol 70:720–728
8. Futagami T, Yamaguchi T, Nakayama S, Goto M, Furukawa K (2006) Effects of chloromethanes on growth of and deletion of the *pce* gene cluster in dehalorespiring *Desulfitobacterium hafniense* strain Y51. Appl Environ Microbiol 72:5998–6003
9. Gerritse J, Drzyzga O, Kloetstra G, Keijmel M, Wiersum LP, Hutson R, Collins MD, Gottschal JC (1999) Influence of different electron donors and acceptors on dehalorespiration of tetrachloroethene by *Desulfitobacterium frappieri* TCE1. Appl Environ Microbiol 65:5212–5221
10. Hasona A, Kim Y, Healy FG, Ingram LO, Shanmugam KT (2004) Pyruvate formate lyase and acetate kinase are essential for anaerobic growth of *Escherichia coli* on xylose. J Bacteriol 186:7593–7600
11. Hrdy I, Muller M (1995) Primary structure and eubacterial relationships of the pyruvate:ferredoxin oxidoreductase of the amitochondriate eukaryote *Trichomonas vaginalis*. J Mol Evol 41:388–396
12. Kaufmann F, Wohlfarth G, Diekert G (1998) *O*-demethylase from *Acetobacterium dehalogenans*—cloning, sequencing, and active expression of the gene encoding the corrinoid protein. Eur J Biochem 257:515–521
13. Lemos RS, Gomes CM, Legall J, Xavier AV, Teixeira M (2002) The quinol:fumarate oxidoreductase from the sulphate reducing bacterium *Desulfovibrio gigas*: spectroscopic and redox studies. J Bioenerg Biomembr 34:21–30
14. Loffler FE, Tiedje JM, Sanford RA (1999) Fraction of electrons consumed in electron acceptor reduction and hydrogen thresholds as indicators of halorespiratory physiology. Appl Environ Microbiol 65:4049–4056
15. Lomans BP, Leijdekkers P, Wesselink JJ, Bakkes P, Pol A, Van Der Drift C, Den Camp HJ (2001) Obligate sulfide-dependent degradation of methoxylated aromatic compounds and formation of methanethiol and dimethyl sulfide by a freshwater sediment isolate, *Parasporobacterium paucivorans* gen. nov., sp. nov. Appl Environ Microbiol 67:4017–4023
16. Mackiewicz M, Wiegel J (1998) Comparison of energy and growth yields for *Desulfitobacterium dehalogenans* during utilization of chlorophenol and various traditional electron acceptors. Appl Environ Microbiol 64:352–355
17. Magnuson JK, Romine MF, Burris DR, Kingsley MT (2000) Trichloroethene reductive dehalogenase from *Dehalococcoides ethenogenes*: sequence of *tceA* and substrate range characterization. Appl Environ Microbiol 66:5141–5147
18. Maillard J, Schumacher W, Vazquez F, Regeard C, Hagen WR, Holliger C (2003) Characterization of the corrinoid iron-sulfur protein tetrachloroethene reductive dehalogenase of *Dehalobacter restrictus*. Appl Environ Microbiol 69:4628–4638
19. Major DW, Mcmaster ML, Cox EE, Edwards EA, Dworatzek SM, Hendrickson ER, Starr MG, Payne JA, Buonamici LW (2002) Field demonstration of successful bioaugmentation to achieve dechlorination of tetrachloroethene to ethene. Environ Sci Technol 36:5106–5116
20. Maymo-Gatell X, Chien Y, Gossett JM, Zinder SH (1997) Isolation of a bacterium that reductively dechlorinates tetrachloroethene to ethene. Science 276:1568–1571
21. Mohn WW, Tiedje JM (1990) Catabolic thiosulfate disproportionation and carbon dioxide reduction in strain DCB-1, a reductively dechlorinating anaerobe. J Bacteriol 172:2065–2070
22. Morita Y, Futagami T, Goto M, Furukawa K (2009) Functional characterization of the trigger factor protein PceT of tetrachloroethene-dechlorinating *Desulfitobacterium hafniense* Y51. Appl Microbiol Biotechnol 83:775–781
23. Morris RM, Sowell S, Barofsky D, Zinder S, Richardson R (2006) Transcription and mass-spectroscopic proteomic studies of electron transport oxidoreductases in *Dehalococcoides ethenogenes*. Environ Microbiol 8:1499–1509
24. Morris RM, Fung JM, Rahm BG, Zhang S, Freedman DL, Zinder SH, Richardson RE (2007) Comparative proteomics of *Dehalococcoides* spp. reveals strain-specific peptides associated with activity. Appl Environ Microbiol 73:320–326
25. Neumann A, Wohlfarth G, Diekert G (1998) Tetrachloroethene dehalogenase from *Dehalospirillum multivorans*: cloning, sequencing of the encoding genes, and expression of the *pceA* gene in *Escherichia coli*. J Bacteriol 180:4140–4145
26. Neumann A, Engelmann T, Schmitz R, Greiser Y, Orthaus A, Diekert G (2004) Phenyl methyl ethers: novel electron donors for respiratory growth of *Desulfitobacterium hafniense* and *Desulfitobacterium* sp. strain PCE-S. Arch Microbiol 181:245–249
27. Nijenhuis I, Zinder SH (2005) Characterization of hydrogenase and reductive dehalogenase activities of *Dehalococcoides ethenogenes* strain 195. Appl Environ Microbiol 71:1664–1667
28. Nonaka H, Keresztes G, Shinoda Y, Ikenaga Y, Abe M, Naito K, Inatomi K, Furukawa K, Inui M, Yukawa H (2006) Complete genome sequence of the dehalorespiring bacterium *Desulfitobacterium hafniense* Y51 and comparison with *Dehalococcoides ethenogenes* 195. J Bacteriol 188:2262–2274
29. Pieulle L, Charon MH, Bianco P, Bonicel J, Petillot Y, Hatchikian EC (1999) Structural and kinetic studies of the pyruvate-ferredoxin oxidoreductase/ferredoxin complex from *Desulfovibrio africanus*. Eur J Biochem 264:500–508
30. Pieulle L, Nouailler M, Morelli X, Cavazza C, Gallice P, Blanchet S, Bianco P, Guerlesquin F, Hatchikian EC (2004) Multiple orientations in a physiological complex: the pyruvate-ferredoxin

oxidoreductase-ferredoxin system. Biochemistry 43:15480–15493
31. Pollock JS, Forstermann U, Mitchell JA, Warner TD, Schmidt HH, Nakane M, Murad F (1991) Purification and characterization of particulate endothelium-derived relaxing factor synthase from cultured and native bovine aortic endothelial cells. Proc Natl Acad Sci U S A 88:10480–10484
32. Prat L, Maillard J, Grimaud R, Holliger C (2011) Physiological adaptation of *Desulfitobacterium hafniense* strain TCE1 to tetrachloroethene respiration. Appl Environ Microbiol 77:3853–3859
33. Ragsdale SW (2004) Life with carbon monoxide. Crit Rev Biochem Mol Biol 39:165–195
34. Rahm BG, Morris RM, Richardson RE (2006) Temporal expression of respiratory genes in an enrichment culture containing *Dehalococcoides ethenogenes*. Appl Environ Microbiol 72:5486–5491
35. Schumacher W, Holliger C (1996) The proton/electron ratio of the menaquinone-dependent electron transport from dihydrogen to tetrachloroethene in *Dehalobacter restrictus*. J Bacteriol 178:2328–2333
36. Seshadri R, Adrian L, Fouts DE, Eisen JA, Phillippy AM, Methe BA, Ward NL, Nelson WC, Deboy RT, Khouri HM, Kolonay JF, Dodson RJ, Daugherty SC, Brinkac LM, Sullivan SA, Madupu R, Nelson KE, Kang KH, Impraim M, Tran K, Robinson JM, Forberger HA, Fraser CM, Zinder SH, Heidelberg JF (2005) Genome sequence of the PCE-dechlorinating bacterium *Dehalococcoides ethenogenes*. Science 307:105–108
37. Smidt H, Song D, Van Der Oost J, De Vos WM (1999) Random transposition by Tn*916* in *Desulfitobacterium dehalogenans* allows for isolation and characterization of halorespiration-deficient mutants. J Bacteriol 181:6882–6888
38. Smidt H, De Vos WM (2004) Anaerobic microbial dehalogenation. Annu Rev Microbiol 58:43–73
39. Stevens TO, Tiedje JM (1988) Carbon dioxide fixation and mixotrophic metabolism by strain DCB-1, a dehalogenating anaerobic bacterium. Appl Environ Microbiol 54:2944–2948
40. Suyama A, Iwakiri R, Kai K, Tokunaga T, Sera N, Furukawa K (2001) Isolation and characterization of *Desulfitobacterium* sp. strain Y51 capable of efficient dehalogenation of tetrachloroethene and polychloroethanes. Biosci Biotechnol Biochem 65:1474–1481
41. Suyama A, Yamashita M, Yoshino S, Furukawa K (2002) Molecular characterization of the PceA reductive dehalogenase of *Desulfitobacterium* sp. strain Y51. J Bacteriol 184:3419–3425
42. Trieber CA, Rothery RA, Weiner JH (1994) Multiple pathways of electron transfer in dimethyl sulfoxide reductase of *Escherichia coli*. J Biol Chem 269:7103–7109
43. Utkin I, Woese C, Wiegel J (1994) Isolation and characterization of *Desulfitobacterium dehalogenans* gen. nov., sp. nov., an anaerobic bacterium which reductively dechlorinates chlorophenolic compounds. Int J Syst Bacteriol 44:612–619
44. Vignais PM, Toussaint B (1994) Molecular biology of membrane-bound $H_2$ uptake hydrogenases. Arch Microbiol 161:1–10
45. Zinder SH, Brock TD (1978) Dimethyl sulfoxide as an electron acceptor for anaerobic growth. Arch Microbiol 116:35–40